

NARROW BANDGAP SEMICONDUCTING SILICIDES: INTRINSIC INFRARED DETECTORS

ON A SILICON CHIP

SBIR - 08.06-4131
release date 10/31/91 ✓Final ReportPrincipal Investigator: Dr. John E. Mahan
(303)491-5509Colorado Research Development Corporation
621 Seventeenth St.
Suite 1620
Denver, CO 80293
(303)293-8633

30 May, 1990

NAS7-994

Project Summary

The main technical objective was to achieve epitaxial growth on silicon of two semiconducting silicides, ReSi_2 and CrSi_2 .

ReSi_2 thin films were grown on (001) silicon wafers by vacuum evaporation of rhenium onto hot substrates in ultrahigh vacuum. The preferred epitaxial relationship was found to be $\text{ReSi}_2(100)/\text{Si}(001)$ with $\text{ReSi}_2[010]||\text{Si}\langle 110 \rangle$. The lattice matching consists of a common unit mesh of 120 \AA^2 area, and a mismatch of 1.8%. Transmission electron microscopy revealed the existence of rotation twins corresponding to two distinct but equivalent azimuthal orientations of the common unit mesh. MeV He^+ backscattering spectrometry revealed a minimum channeling yield of 2% for a $\sim 1,500 \text{ \AA}$ thick film grown at 650 C. Although the lateral dimension of the twins is on the order of 100 \AA , there is a very high degree of alignment between the $\text{ReSi}_2(100)$ and the $\text{Si}(001)$ planes.

Highly oriented films of CrSi_2 were grown on (111) silicon substrates, with the matching crystallographic faces being $\text{CrSi}_2(001)/\text{Si}(111)$. The reflection high-energy electron diffraction (RHEED) patterns of the films consist of sharp streaks, symmetrically arranged. The predominant azimuthal orientation of the films was determined to be $\text{CrSi}_2\langle 210 \rangle || \text{Si}\langle 110 \rangle$. This highly desirable heteroepitaxial relationship has been obtained previously by others; it may be described with a common unit mesh of 51 \AA^2 and a mismatch of 0.3%. RHEED also revealed the presence of limited film regions of a competing azimuthal orientation, $\text{CrSi}_2\langle 110 \rangle || \text{Si}\langle 110 \rangle$. A channeling effect for MeV He^+ ions was not found for this material.

Potential commercial applications of this research may be found in silicon-integrated infrared detector arrays. Optical characterizations showed that semiconducting ReSi_2 is a strong absorber of infrared radiation, with the absorption constant increasing above $2 \times 10^4 \text{ cm}^{-1}$ for photon energies above 0.2 eV. CrSi_2 is of potential utility for detection at photon energies above $\sim 0.3 \text{ eV}$.

(NASA-CR-190882) NARROW BANDGAP
SEMICONDUCTING SILICIDES: INTRINSIC
INFRARED DETECTORS ON A SILICON
CHIP Final Report (Colorado
Research Development Corp.) 24 p

N93-13430

Unclass

Introduction

The first and foremost technical objective was to achieve epitaxial growth on silicon of the two semiconducting silicides, ReSi_2 and CrSi_2 .

Superb growth results were obtained with ReSi_2 , with respect to the quality of the epitaxial alignment, and from the standpoint of fundamental scientific interest. ReSi_2 grown on (001)Si wafers exhibited an RBS channeling yield of 2%, with the right growth conditions. Detailed analysis of the channeling phenomenon yielded new insights pertaining to polyatomic epitaxial films.

CrSi_2 epitaxy, on the other hand, remains an enigma. It offers an excellent theoretical lattice match to (111)Si, better than ReSi_2 on (001)Si, but experimentally has not exhibited excellent large-area epitaxy. We find two competing azimuthal orientations of the films.

Optical analysis of ReSi_2 showed that it is a strong absorber of infrared radiation at and above photon energies of 0.2 eV. Attempts to measure photoelectronic properties of the films did not meet with success.

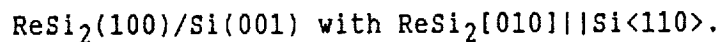
A considerable amount of work during the project went into developing experimental procedures, including substrate preparation, interpretation of RHEED patterns, and optical analysis of the samples. We report below our principal technical results, within the context of recent related work:

I. ReSi_2 Technical Results

ReSi_2 has been shown recently to possess an orthorhombic lattice which is very nearly tetragonal, with lattice parameters $a = 3.128 \text{ \AA}$, $b = 3.144 \text{ \AA}$, and $c = 7.677 \text{ \AA}$.¹ (To simplify the following discussion, we shall assume that the material is tetragonal with the lattice parameters $a = b = 3.13 \text{ \AA}$.) For the growth of ReSi_2 on the Si(001) face there is no simple lattice parameter match in the conventional sense. However, an acceptable "lattice matching" is still achievable via the formation of a coincidence net, with a reasonably-sized unit mesh common to the matching faces of the two materials.^{2,3}

According to Zur et al.⁴, the smallest unit mesh with less than 3.0% mismatch for ReSi_2 on a (001) silicon substrate is 119 \AA^2 in size, for the $\text{ReSi}_2(110)$ face. Chu et al. have reported "localized epitaxy" for ReSi_2 on (001) silicon, finding this matching face relationship but with two competing and nonequivalent azimuthal orientations.⁵

There exists another epitaxial relationship possessing a common unit mesh of a similar size. It is 120 \AA^2 in area and has a room temperature mismatch of +1.8% along $\text{ReSi}_2[010]$ but only -0.03% along $\text{ReSi}_2[001]$. The epitaxial relationship is



The common unit mesh consists of five primitive unit meshes of the $\text{ReSi}_2(100)$ face and of eight primitive unit meshes of the Si(001) face. There are two

distinct but equivalent azimuthal orientations of this common unit mesh. As shown in Figure 1, they differ by an azimuthal rotation of 90° about the silicide [100] axis. This lattice match is also included in Zur et al.'s tables.⁴ We will show below that the epitaxial relationship shown in Figure 1 is very strongly preferred in the samples we have grown.

We grew ReSi_2 thin films on (001) silicon wafers by depositing pure rhenium metal onto hot substrates. To prepare the substrate surface, the wafer was removed from the box, etched for thirty seconds in buffered HF solution, and loaded immediately into the sample introduction chamber of the growth system. After its transfer into the growth chamber, the wafer was held at 400 C for fifteen minutes. During this step we typically observe the development of strong Kikuchi streaks and the 2×2 reconstructed reflection high energy electron diffraction (RHEED) pattern of the silicon (001) surface. The substrate preparation was concluded with a "silicon beam clean," during which any remaining SiO_2 was etched by a low level silicon flux.⁶ The silicon beam clean consists of the exposure of the surface to a silicon flux corresponding to a deposition rate of 0.2 A/s for 250 s at 700 C. This irradiation of the wafer surface by the low level silicon flux results in an even sharper and brighter RHEED pattern, suggesting that an atomically clean and essentially planar surface exists for the subsequent silicide growth.

High purity rhenium (99.99%) was deposited from an electron beam evaporation source, with the silicon for silicide formation being supplied by the substrate. During the growth, the preselected substrate temperature was maintained with a graphite heater, a feedback controller, and a tungsten-rhenium thermocouple near to or touching the back side of the rotating substrate. Although the system's base pressure is in the 10^{-11} torr range, the pressure was typically in the mid- 10^{-9} torr range during growth. Compositional analysis by Auger depth profiling indicated that there were no detectable impurities within the interior of the films.

The preferred matching face relationship of $\text{ReSi}_2(100)/\text{Si}(001)$ was observed over a wide range of growth temperature, from 400 to 1,000 C. To illustrate this, we show in Figure 2 a Bragg-Brentano X-ray diffraction pattern which was obtained from a $\sim 1,500$ A ReSi_2 film grown at 650 C. This technique samples the crystalline planes which are parallel to the surface of the substrate. The ReSi_2 copper k-alpha (200) reflection at 59.0° is very intense, being similar in strength to the silicon substrate's (400) peak at 69.1° . Due to incomplete removal of the copper k-beta radiation by our nickel filter, the Si(400) k-beta peak at 61.7° is also present. No other film reflections are seen in the diffraction pattern; this indicates a very pure matching face relationship.

MeV He^+ backscattering spectrometry was used to quantitatively assess the degree of epitaxy between the film and the substrate. Backscattering spectra for both random and $\text{Si}\langle 001 \rangle$ -aligned beam incidence are shown in Figure 3. The ratio of the aligned to random backscattering yields (X_{min}) for the metal, at an energy (~ 1.25 MeV here) just to the left of the surface peak, is commonly used as a quantitative indicator of the crystalline perfection of epitaxial films. Values of X_{min} on the order of 3-5% are observed for structurally excellent epitaxial films of other transition metal silicides.⁷

The spectra in Figure 3, which were obtained for a film grown at 650 C,

give a X_{\min} value of 2%. This result indicates an excellent alignment of the film as viewed along the silicon [001] direction. The minimum yield of the silicon signal from the film (~14%) greatly exceeds that of rhenium. This does not reflect an enhanced imperfection of the silicon sublattice in ReSi_2 , but is an artifact of channeling in this material.⁸ The peak in the aligned spectrum that corresponds to the film/substrate interface (near 1.1 MeV) is caused by misfit dislocations and indicates that the film is not pseudomorphic. The thickness and the atomic composition of the film were determined from the random spectrum. The Si/Re atomic ratio is 1.9 ± 0.1 , which is consistent with the expected stoichiometric composition. Thus, X-ray diffraction and channeling measurements both indicate an excellent alignment of the $\text{ReSi}_2(100)$ and $\text{Si}(001)$ planes.

Transmission electron microscopy and diffraction were used to characterize the lateral microstructure of the films and to determine the relative azimuthal orientation of the film with respect to the substrate. A bright-field plan-view micrograph and a transmission electron diffraction pattern for the film of Figure 3 are shown together in Figure 4.

The transmission electron diffraction pattern (shown as an inset in Figure 4) contains diffraction spots from both the ReSi_2 film and the silicon substrate, with those of the latter being particularly bright. The presence of sharp diffraction spots from the film suggests that it is highly aligned to the substrate. Since the (100) face of ReSi_2 possesses only twofold symmetry, the fourfold symmetry of the observed film pattern suggests that regions of differing azimuthal orientation are present within the film.

These regions are rotation twins, which are a consequence of the two distinct but equivalent azimuthal orientations of the common unit mesh.⁹ Indeed, the complete transmission electron diffraction pattern may be predicted by superposing the silicon pattern with those of two (assumed equally probable) rotation twins in the film. The required relative orientation of the twins' diffraction patterns with respect to that of the substrate shows that the twins are azimuthally aligned as predicted above: $\text{ReSi}_2[010]||\text{Si}\langle 110 \rangle$. With this finding, the epitaxial orientation was completely established.

We find that films grown at 650 C by reactive deposition epitaxy consist entirely of such twins in apparently equal numbers. Bright field plan view transmission electron microscopy (Figure 4) shows that their lateral extent is very small, on the order of 100 Å. It is a matter of considerable interest that, in spite of the very small lateral dimension of the rotation twins, a very good He^+ channeling yield was observed.

Optical properties, normal incidence transmittance and reflectance, were measured for some epitaxially oriented films as described above. The index of refraction and extinction coefficient were obtained as functions of photon energy. A representative value of the index is 3.7, although it varies somewhat as a function of photon energy. The optical absorption coefficient was calculated from the extinction coefficient and the results are shown in Figure 5. There is a considerable amount of extrinsic absorption at low energies, but it appears that the intrinsic absorption coefficient of the material is seen above 0.2 eV. The material is quite a strong absorber of infrared radiation, as can be seen from the Figure.

We tried to observe photoelectronic properties of the epitaxial films, but could not do so. Mesa structures were fabricated. An evaporated nickel film was patterned and used as an etch mask for the ReSi_2 film. The nickel was impervious to a $\text{CF}_4 + \text{O}_2$ plasma which nicely etched the silicide, and it also served as a low resistance contact to ReSi_2 .

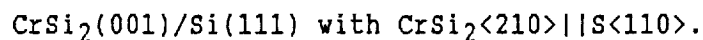
Rectifying heterojunctions were obtained. A representative current-voltage characteristic is shown in Figure 6. The heterojunction mesa structure thus created showed a photoresponse only when the photon energy was greater than that corresponding to the silicon bandgap. Thus, we could not detect a photoresponse that was attributable to the semiconducting silicide itself, even with a very sensitive lock-in amplifier and light chopper.

II. CrSi_2 Technical Results

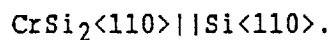
The quest for epitaxial CrSi_2 films on silicon has attracted more attention than that of perhaps any other semiconducting silicide.¹⁰⁻¹³ This effort was encouraged by a promising theoretical lattice match of the hexagonal CrSi_2 basal planes to the $\text{Si}(111)$ face.³ There is a possible common unit mesh of 51.1 \AA^2 area with a mismatch of 0.3% for the so-called "Type A" azimuthal orientation.¹⁴

It has proved difficult to obtain single crystal films because for the same matching face relationship, there is an alternative azimuthal orientation that competes effectively with Type A. For this "Type B" azimuthal orientation¹⁴, a possible common unit mesh may be identified that has an area of only 17 \AA^2 . However, the mismatch is 15.3%. This relatively poor mismatch value makes it seem unlikely that the Type B orientation could in fact be a viable alternative, but it is. To summarize the experimental situation, it is generally observed that the predominant matching face relationship to (111) silicon is constant over a fairly wide range of film growth temperatures, but that the films consist of regions of both orientations.

The specification of the heteroepitaxial relationship with the Type A azimuthal orientation is



The Type B azimuthal orientation represents a rotation of the film of 30° about the direction normal to the substrate's surface, to achieve the following alignment:



In Figure 7, against the background of the crystalline net of the (111) silicon face, we show the primitive unit mesh of the $\text{CrSi}_2(001)$ face in each of the two above-mentioned azimuthal orientations, with the two possible common unit meshes. Their areas are indicated. For the Type B orientation, the silicide's own primitive unit mesh is shown as the common unit mesh; for the Type A orientation, the common unit mesh is the size of three primitive silicide unit meshes or essentially four silicon unit meshes. Some pertinent distances, from which the mismatches were calculated, are also shown. It is

customary to calculate the mismatch using the substrate dimension as the reference, and the common unit mesh area using the silicide dimensions.⁴ We have described the relative orientations of the silicide and silicon crystalline lattices, but should emphasize that their relative positions are unknown.

We grew CrSi_2 thin films on (111) silicon wafers by evaporation of the pure metal (99.95%) onto hot substrates under ultra-high vacuum. The silicon for silicide formation was supplied by the substrate. Substrate surface preparation was the same as for ReSi_2 growth.

The preferred matching face relationship, $\text{CrSi}_2(001)/\text{Si}(111)$, was confirmed with data such as that shown in Figure 8. This is a copper k-alpha Bragg-Brentano X-ray diffraction pattern from a sample grown by depositing 1000 Å of chromium at 400 C. Only one CrSi_2 film peak is seen, the (003) reflection at 42.6° . In addition, there are strong substrate reflections (which include "structure factor-forbidden" reflections and k-beta reflections) as identified in the Figure.

Since the technique samples crystalline planes which are parallel to the macroscopic surface of the silicon wafer, a preference for the above matching face relationship is demonstrated. In a survey of growth temperature effects, we observed that the $\text{CrSi}_2(003)$ peak was dominant at temperatures of 800 C and below. Although the 400 and 500 C growths gave clean X-ray patterns, temperatures of 600 C and above resulted in a loss of purity of the matching face relationship, with the $\text{CrSi}_2(111)$ reflection and some others appearing.

We will present RHEED patterns which were obtained from a film grown by depositing 300 Å of chromium at 600 C, and given a post-growth anneal at 900 C. While some loss of purity of the matching face relationship occurred at this growth temperature (as just noted), the basic structure of the RHEED patterns was invariant with growth temperatures from 400 to 600 C. The 900 C post-growth anneal did not alter the epitaxial relationship of the as-grown film, but brought forth the highest quality RHEED patterns, in terms of streak sharpness and brightness.

We show in Figure 9 two RHEED patterns which were observed with the incident beam (a) along a $\text{Si}\langle 110 \rangle$ direction and (b) along a $\langle 112 \rangle$ direction. The lateral streak spacings on the RHEED screen were 17 and 10 mm, respectively. Each pattern was repetitive with an azimuthal rotation of the sample by some multiple of 60° .

These streaks are bright and sharp, and of a similar quality to those obtained from a clean $\text{Si}(111)$ surface. The RHEED pattern suggests to us that the CrSi_2 surface is well-ordered on a scale at least as large as the coherence length of the electron beam (~ 100 Å) and sufficiently smooth that there is no transmission electron diffraction pattern seen, as is often the case with rough but epitaxial films.

It is possible to use this streak pattern to determine the azimuthal orientation of the film. The RHEED streak spacing that is expected for various incident beam directions may be calculated from the reciprocal net of the $\text{CrSi}_2(001)$ face. For certain principal directions there will be zones of reciprocal lattice rods with a particular intrarow rod spacing, a^* . These

zones will create streaks on the RHEED screen having a spacing (W) given by

$$W = \lambda La^*/2 \quad , \quad (1)$$

where λ is the deBroglie wavelength of the incident electrons and L is the distance from the point of incidence on the sample surface to the RHEED screen.¹⁵

The crystalline surface net of the CrSi₂ (001) face, from which we will derive the reciprocal net and the expected RHEED streak spacings, is shown in Figure 10. Some principal crystallographic directions are indicated. Common choices for the basis vectors of the crystalline net and other relevant quantities are given in Table I. The Cartesian unit vectors, with which the basis vectors are expressed, are shown in Figure 10.

The basis vectors of the reciprocal net (\bar{a}_i^*) are derived from those of the real crystalline net (\bar{a}_i) according to

$$\bar{a}_1^* = 2\pi \bar{a}_2 \times \bar{n}/A \quad (2)$$

and

$$\bar{a}_2^* = 2\pi \bar{n} \times \bar{a}_1/A \quad (3)$$

with

$$A = \bar{a}_1 \cdot \bar{a}_2 \times \bar{n}. \quad (4)$$

\bar{n} is a unit vector normal to the surface and A is the area of the crystalline unit mesh.¹⁶ \bar{n} , A, and the resulting reciprocal net basis vectors are also given in Table I. Both the crystalline net and the reciprocal net of the CrSi₂(001) face are close-packed hexagonal arrays. However, their orientations differ by a rotation of 30°, as drawn in Figure 10.

One may see in Figure 9 that for an incident RHEED beam direction along CrSi₂<100> or <110>, the intrarow rod spacing of the Zeroth Zone would be 1.638 Å⁻¹. Along CrSi₂<120>, it is $\sqrt{3}$ times this value, or 2.837 Å⁻¹. Our RHEED screen distance is roughly 3.1 X 10⁻¹ m and the electron wavelength corresponding to our acceleration voltage of 10 kV is 0.122 eV. The expected RHEED streak spacings, according to Equation 1, are 10 and 17 mm, respectively, for the two rod spacings.

The expected RHEED streak spacings agree with the observed values to within experimental error. Moreover, a Type A azimuthal orientation of the film is strongly suggested. A match is obtained between the experimental and predicted streak spacings with CrSi₂<100> or <110> parallel to Si<112> and with CrSi₂<210> parallel to Si<110>. For the Type B orientation, the streak spacings would simply be interchanged.

A close examination of Figure 9a shows a rather weak "extra" streak on the left side and possibly one on the right, as well, which have been ignored in the preceding discussions. Our interpretation is that this is actually a composite RHEED pattern, due to the presence of film regions of the Type B azimuthal orientation as well as Type A. These extra streaks are at the positions of two of the streaks of Figure 9b. Thus, it appears that the film is essentially of the Type A orientation, but enough Type B is present to generate the extra streaks seen in Figure 9a. With a growth temperature of typically 400 C, the RHEED pattern is a most definitely a composite,

consisting of strong representations of both patterns of Figure 3, and is identical for both incident beam directions.

We would like to comment briefly on the epitaxial quality of the films. Transmission electron microscopy has not confirmed the existence of large-area single-crystal films, for any growth temperature we tried. It seems that strong, sharp RHEED streak patterns are obtainable from films that are not necessarily of a large-area single-crystal structure.

We have characterized the Type B azimuthal orientation with a common unit mesh of 17 \AA^2 area and a mismatch of 15.3%. This mesh area is quite small (and therefore quite good) but the mismatch is so large that one might not expect any natural preference for this orientation. Yet it has been observed by several investigators and we have strong evidence for its existence in our RHEED patterns.

There is another possible lattice matching for this heteroepitaxial relationship which may be more convincing. We show in Figure 11 the crystalline net of the $\text{CrSi}_2(001)$ face, its primitive unit mesh, and an alternative common unit mesh against the unit mesh of the $\text{Si}(111)$ face, oriented to correspond to Type B. It has an area of 612 \AA^2 and a mismatch of only 1.2%. This mismatch value would be considered promising but there could be some doubt about the workability of such a large common unit mesh. One may gain a perspective by considering the unit mesh of the reconstructed $\text{Si}(111)7 \times 7$ surface. It is identical to that shown in Figure 11. We reason that if a unit mesh of 612 \AA^2 is workable for the most commonly observed reconstruction of the $\text{Si}(111)$ surface, it may be suitable as well for the alignment of this heteroepitaxial system.

III. Estimates of Technical Feasibility

The X-ray diffraction data and the very low values of X_{\min} for the ReSi_2 films might lead one to think that they are of a single crystal structure. However, the TEM analysis clearly shows that rotation twins do coexist. The very pure matching face relationship that we have observed suggests that modest improvements in the growth technique may lead to material of a quality sufficient for optoelectronic device development. Perhaps devices in which charge transport is in the vertical direction will be possible with the present type of film microstructure. It may yet be possible to grow truly single-crystal films by optimizing the growth kinetics or the substrate preparation.

It is well-established now that CrSi_2 films grow on clean $\text{Si}(111)$ surfaces with a strong preference for the matching face relationship of $\text{CrSi}_2(001)/\text{Si}(111)$. Under the right conditions, the films exhibit symmetric RHEED patterns with very sharp streaks. The streak spacings observed for various incident beam directions agree with those calculated for the $\text{CrSi}_2(001)$ face. Thus, RHEED patterns may be used to determine the azimuthal orientation of the film with respect to the substrate. For the samples discussed in this paper, the highly desirable "Type A" azimuthal orientation, $\text{CrSi}_2\langle 210 \rangle \parallel \text{Si}\langle 110 \rangle$, predominated.

RHEED also showed the presence of CrSi_2 film regions of the "Type B"

orientation. The theoretical justification of this orientation was strengthened with the observation that the unit mesh of the reconstructed Si(111)7X7 surface is a possible common unit mesh pertaining to this azimuthal orientation. The relative importance of the two factors in the lattice matching tradeoff (common unit mesh areas and mismatch) are not well understood, nor are their absolute limits.

We are optimistic that it will be possible to find a way to control the azimuthal orientation of CrSi₂ grown on (111)Si, creating large-area single-crystal films.

References

1. T. Siegrist, F. Hulliger, and G. Travaglini, *J. Less-Common Metals*, 92, 119 (1983).
2. A. Zur and T.C. McGill, *J. Appl. Phys.* 55(2), 378 (1984).
3. A. Zur, T.C. McGill, and M-A. Nicolet, *J. Appl. Phys.* 57(2), 600 (1985).
4. A. Zur, T. McGill, and M. Nicolet, "Tables of Lattice Matches between Transition Metal Silicides and Silicon," Physics Auxiliary Publication Service, American Institute of Physics, Doc. No. JAPIA-57-0600-76 (1984).
5. J.J. Chu, L.J. Chen, and K.N. Tu, *J. Appl. Phys.* 63(2), 461 (1987).
6. K. Kugimiya, Y. Hirofujii, and N. Matsuo, *Jap. J. Appl. Phys.*, Vol. 24, No. 5, 564 (1985).
7. S. Saitoh, H. Ishiwara, T. Asano, and S. Furukawa, *Jap. J. Appl. Phys.*, Vol. 20, No. 9, 1649 (1981).
8. G. Bai, M-A. Nicolet, T. Vreeland, J. Mahan, K. Geib, and G.Y. Robinson (unpublished).
9. C. Barrett and T.B. Massalski, Structure of Metals, 3rd Rev. Ed. (Pergamon, Oxford, 1980), 406.
10. V.G. Lifshits, V.G. Zavodinskii, and N.I. Plyusnin, "Formation of Surface Chromium Phases and CrSi₂ Epitaxy on Si(111), *Phys. Chem. Mech. Surfaces*, Vol. 2(3), 784 (1984).
11. F.Y. Shiau, H.C. Cheng, and L.J. Chen, "Localized Epitaxial Growth of CrSi₂ on Silicon," *J. Appl. Phys.* 59(8), 2784 (1986).
12. R.W. Fathauer, P.J. Grunthner, T.L. Lin, K.T. Chang, J.H. Mazur, and D.N. Jamieson, "Molecular-Beam Epitaxy of CrSi₂ on Si(111)," *J. Vac. Sci. Technol.* 6(2), 708 (1988).
13. L. Haderbache, P. Wetzel, C. Pirri, J.C. Peruchetti, D. Bolmont, and G. Gewinner, "Molecular Beam Epitaxy of Monotype CrSi₂ on S(111), *Surf. Sci.* 209, L139 (1989).
14. R.W. Fathauer, P.J. Grunthner, T.L. Lin, K.T. Chang, and J.H. Mazur, "Nucleation and Growth of CrSi₂ on Si(111)," *Mat. Res. Soc. Symp. Proc.*, Vol. 116, 453 (1988).
15. John E. Mahan, Kent M. Geib, G.Y. Robinson, and Robert G. Long, "A Review of the Geometrical Fundamentals of Reflection High-Energy Electron Diffraction with Application to Silicon Surfaces," to be published in *J. Vac. Sci. Tech.*.
16. D.P. Woodruff and T.A. Delchar, Modern Techniques of Surface Science (Cambridge University Press, Cambridge, 1986), p. 24.

TABLE I

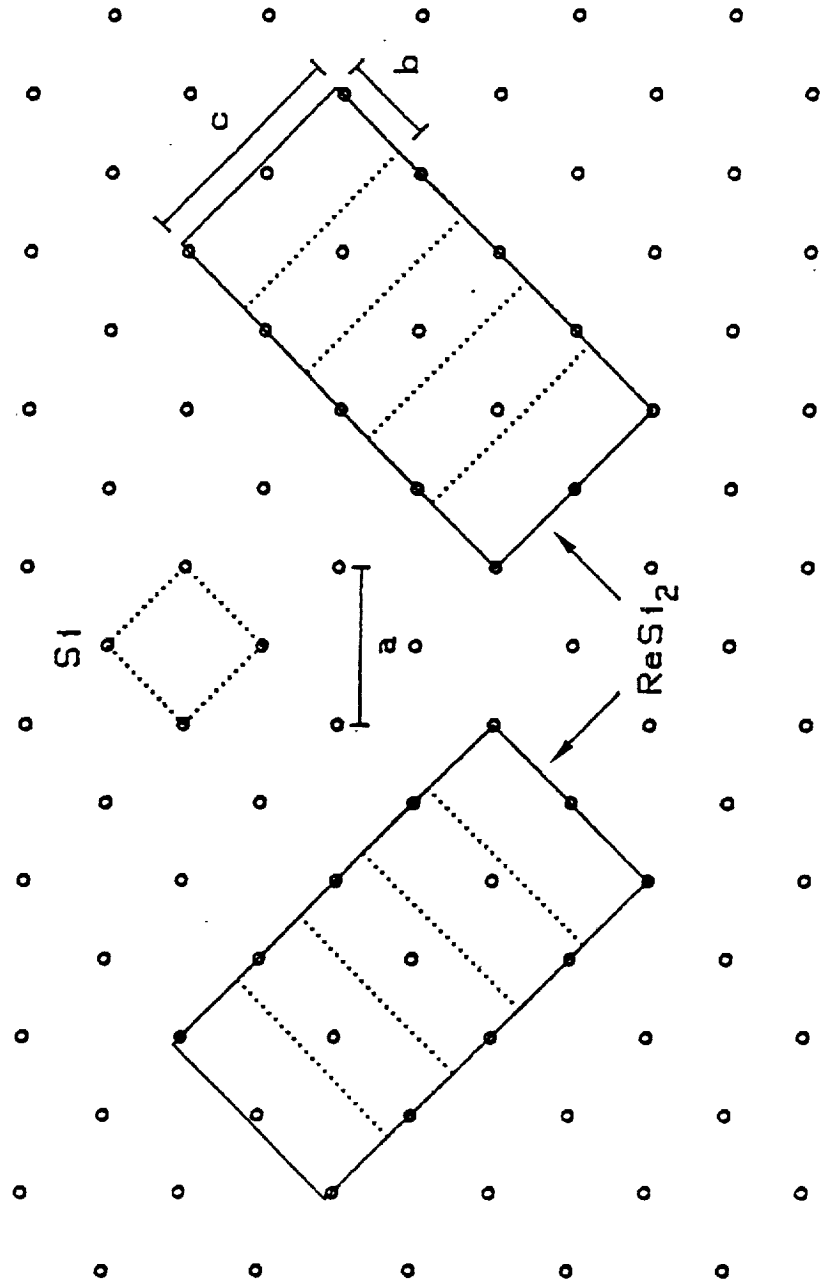
STRUCTURAL PARAMETERS FOR THE CrSi_2 (001) FACE

Unit Vector Normal to the Surface	$\bar{n} = (0,0,1)$
Area of Primitive Unit Mesh	$A = 16.98 \text{ angstroms}^2$
Basis Vectors of Crystalline Net	$\bar{a}_1 = 4.428(\sqrt{3}/2, -1/2, 0) \text{ angstroms}$ $\bar{a}_2 = 4.428(0, 1, 0)$
Basis Vectors of Reciprocal Net	$\bar{a}_1^* = 1.638(1, 0, 0) \text{ angstroms}^{-1}$ $\bar{a}_2^* = 1.638(1/2, \sqrt{3}/2, 0)$

Figure Captions

1. The predicted common unit mesh for $\text{ReSi}_2(100)$ on the $\text{Si}(001)$ face, together with the primitive unit mesh of each material. The fcc lattice parameter of silicon (a) and the tetragonal lattice parameters for ReSi_2 in the plane of the interface (b and c) are also shown. There are two distinct but equivalent azimuthal orientations of this common unit mesh. The actual position of the rectangular ReSi_2 mesh with respect to the silicon square mesh is an assumed one; only their relative orientations are known. The room temperature mismatch along $\text{ReSi}_2[010]$ is clearly visible.
2. A Bragg-Brentano X-ray diffraction pattern for a film grown at 650 C. The film thickness is $\sim 1,500$ Å.
3. 1.4 MeV He^+ backscattering spectra of the ReSi_2 film of Figure 2 for random and for $\text{Si}[001]$ -aligned beam incidence. The scattering angle of the detected particles is 170° .
4. A bright-field plan-view transmission electron micrograph for a ReSi_2 film grown at 700 C. A transmission electron diffraction pattern is shown as an inset. The 100 keV incident electron beam was aligned with $\text{Si}[001]$.
5. Optical absorption coefficient of a representative ReSi_2 film, as a function of photon energy.
6. Current-voltage characteristic of a representative ReSi_2 -Si mesa heterostructure.
7. Possible common unit meshes of the Types A and B azimuthal orientations for $\text{CrSi}_2(001)/\text{Si}(111)$.
8. A Bragg-Brentano X-ray diffraction pattern for a CrSi_2 film grown by depositing 1000 angstroms of chromium onto a (111) silicon wafer at 400 C.
9. CrSi_2 RHEED patterns with the incident beam along the substrate directions (a) $\text{Si}\langle 110 \rangle$ and (b) $\text{Si}\langle 112 \rangle$. The film was prepared by depositing 300 angstroms of chromium at 600 C. The RHEED patterns were obtained after a post-deposition anneal at 900 C.
10. The crystalline net and the reciprocal net of the $\text{CrSi}_2(001)$ surface. The Cartesian unit vectors, which were used to express the basis vectors, are shown.
11. An alternative common unit mesh for the Type B azimuthal orientation.

THE TWO POSSIBLE AZIMUTHAL ORIENTATIONS
 OF THE COMMON UNIT MESH
 $\text{ReSi}_2(100)/\text{Si}(001)$ WITH $\text{ReSi}_2[010] \parallel \text{Si}\langle 110 \rangle$



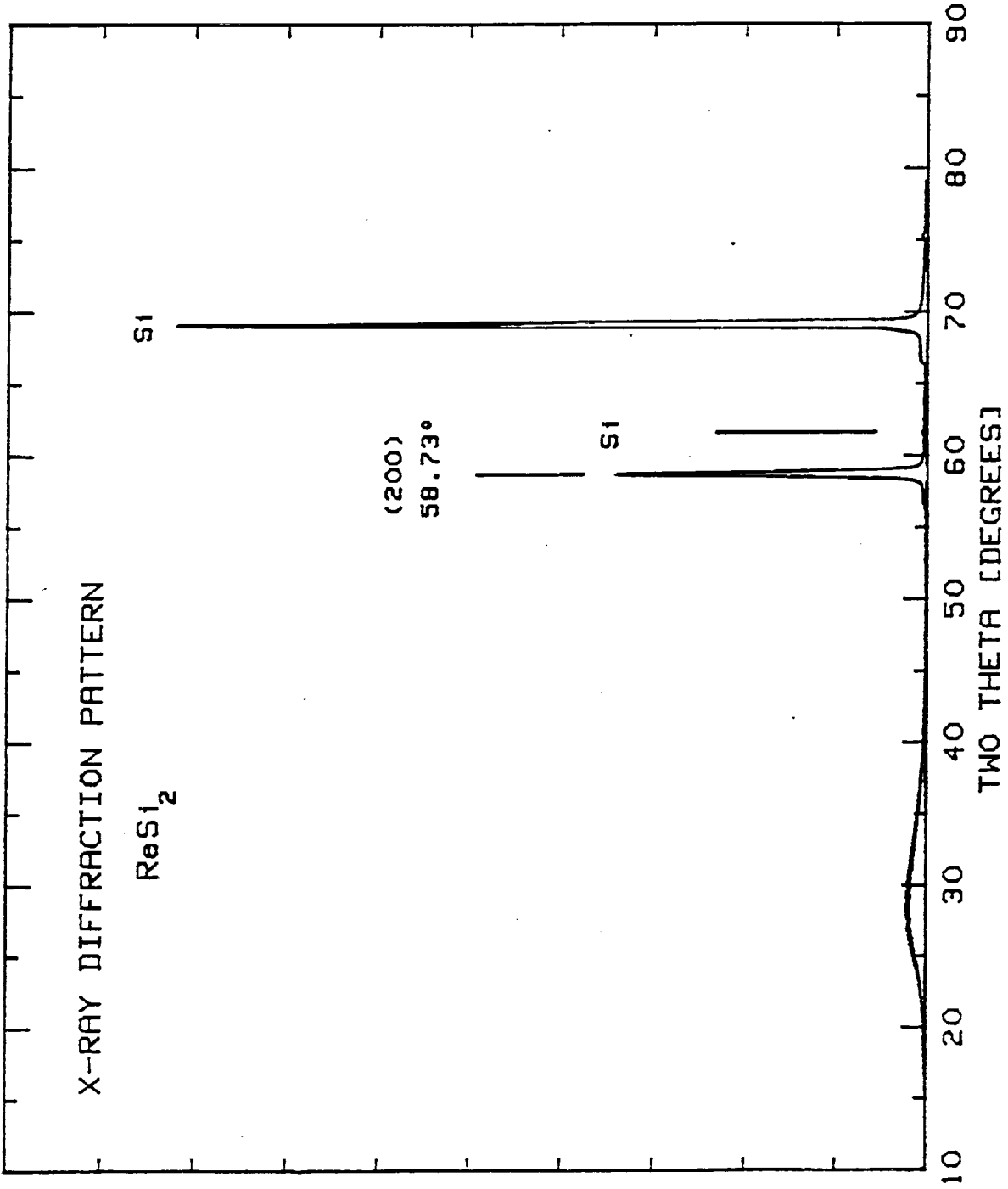


Fig. 2

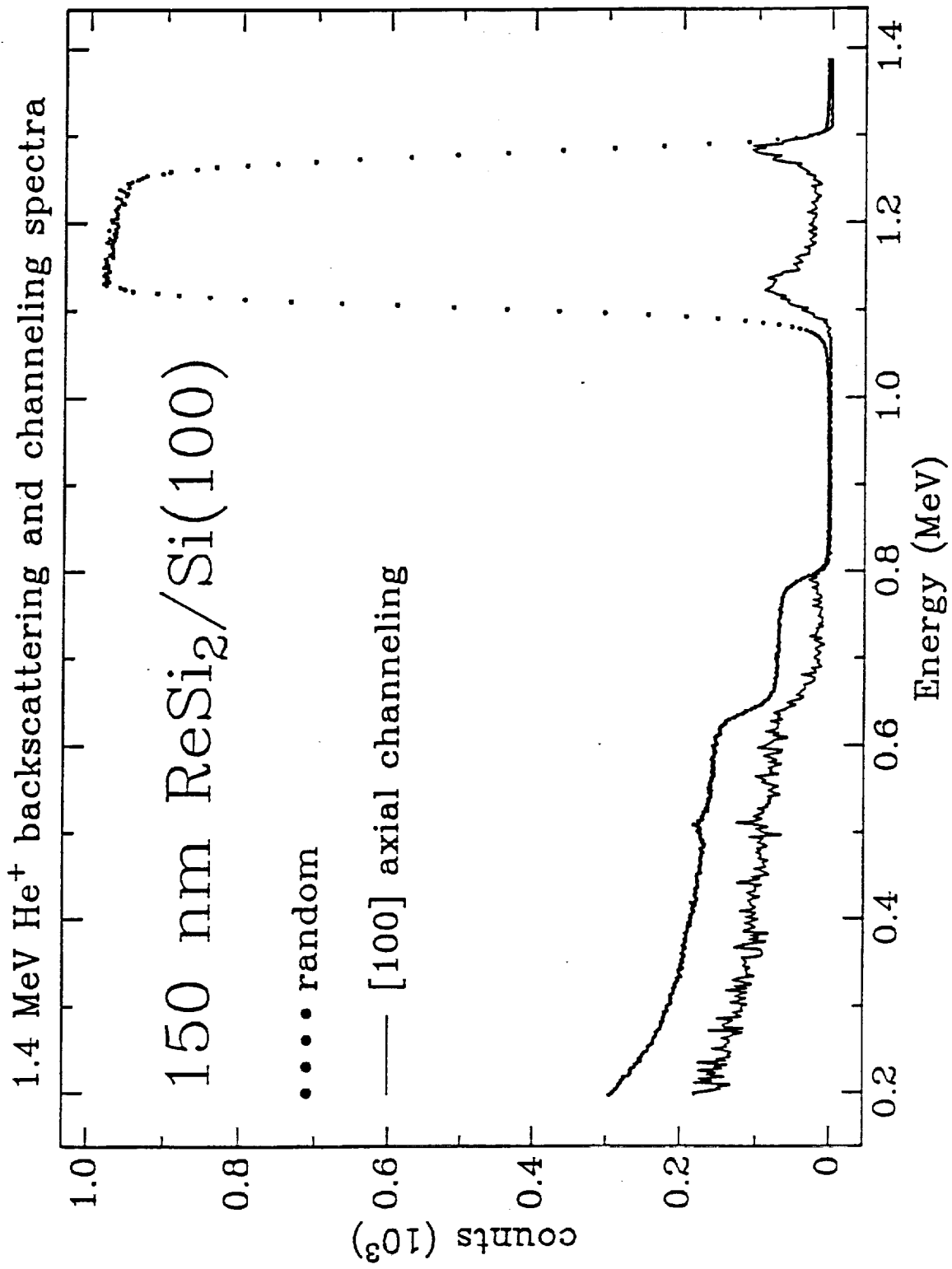
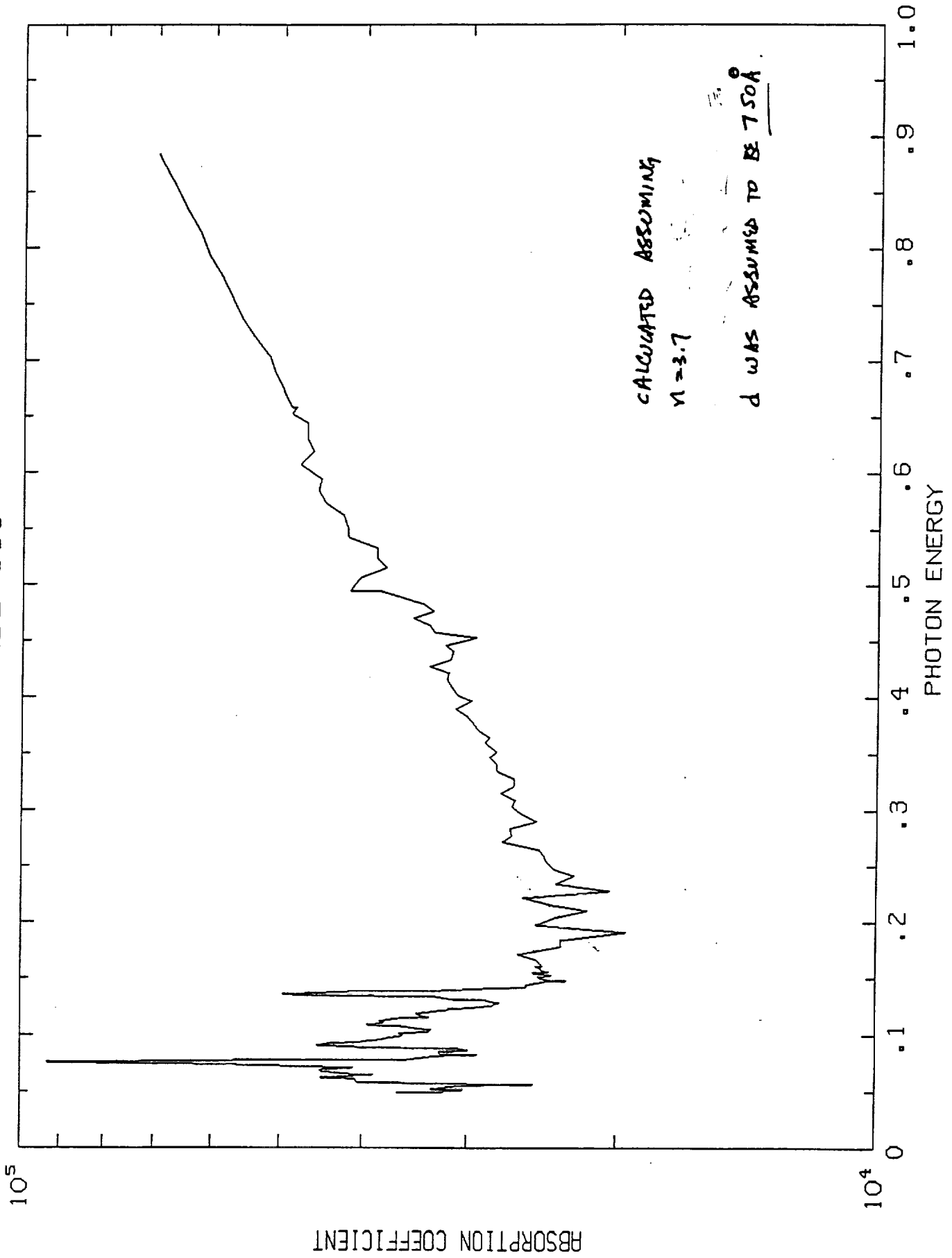


Fig. 3



Fig. 4

MBE-153



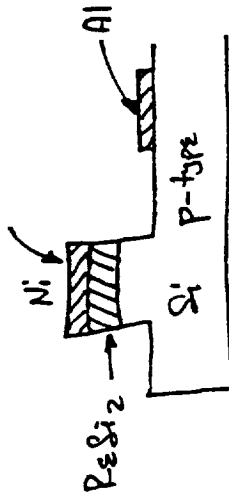
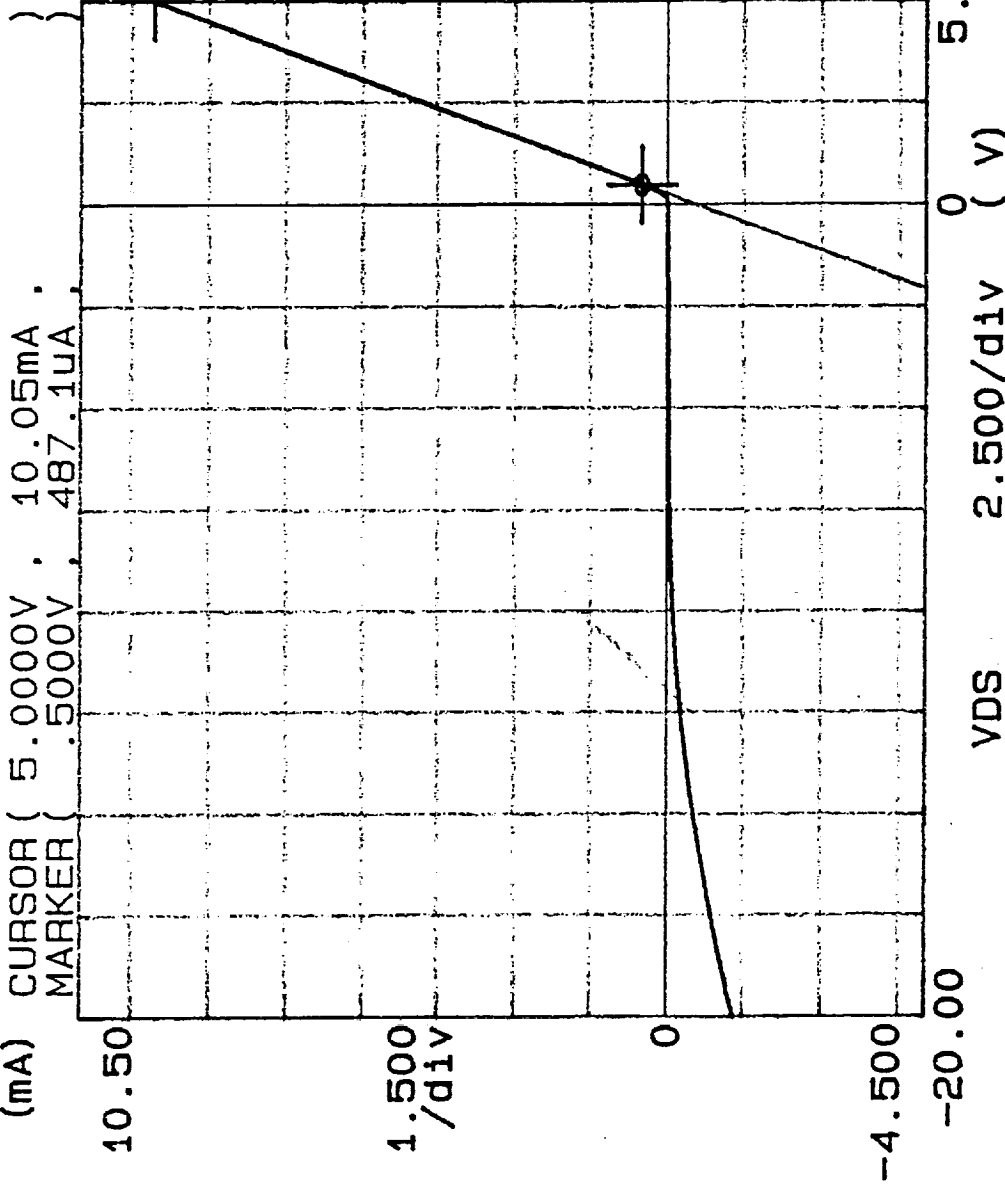
***** GRAPHICS PLOT *****

MBE-155-RE NI MESAS

NO ILLUMINATION, DARK CURRENT

ID (mA) CURSOR (5.0000V ; 10.05mA .

MARKER (.5000V ; 487.1uA .



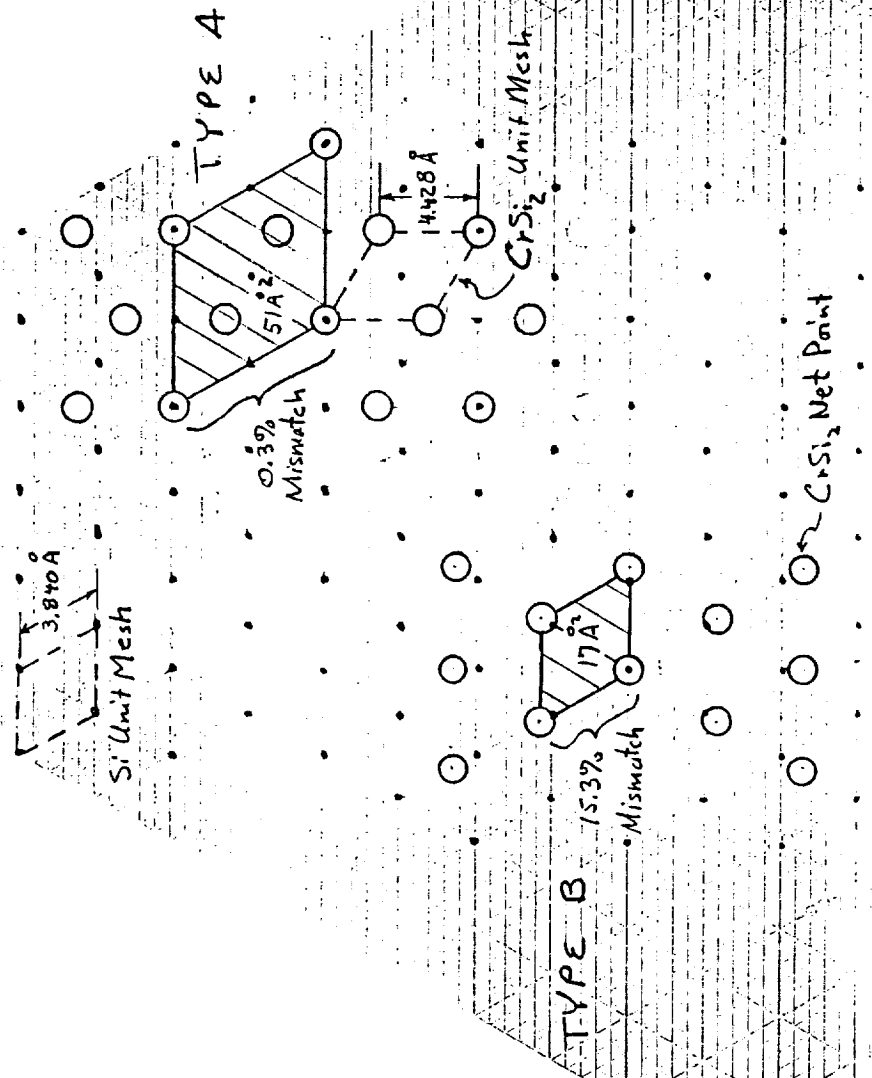
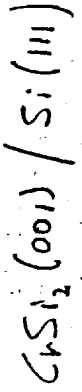
115.3

100

0

Letters stream line of
last — high

POSSIBLE COMMON UNIT MESHES



100

115.3

HP FILENUMBER US 800028

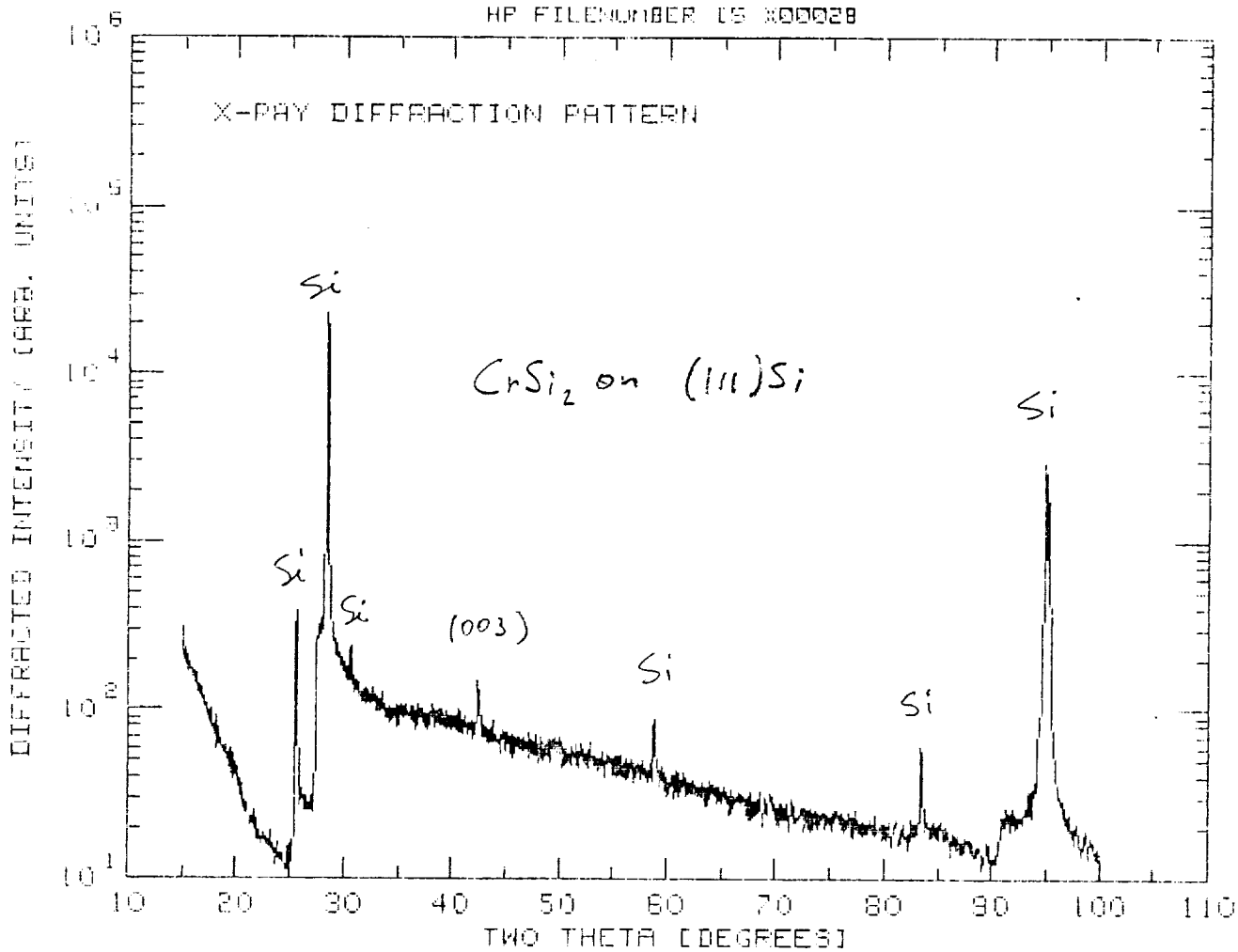


Fig. 8

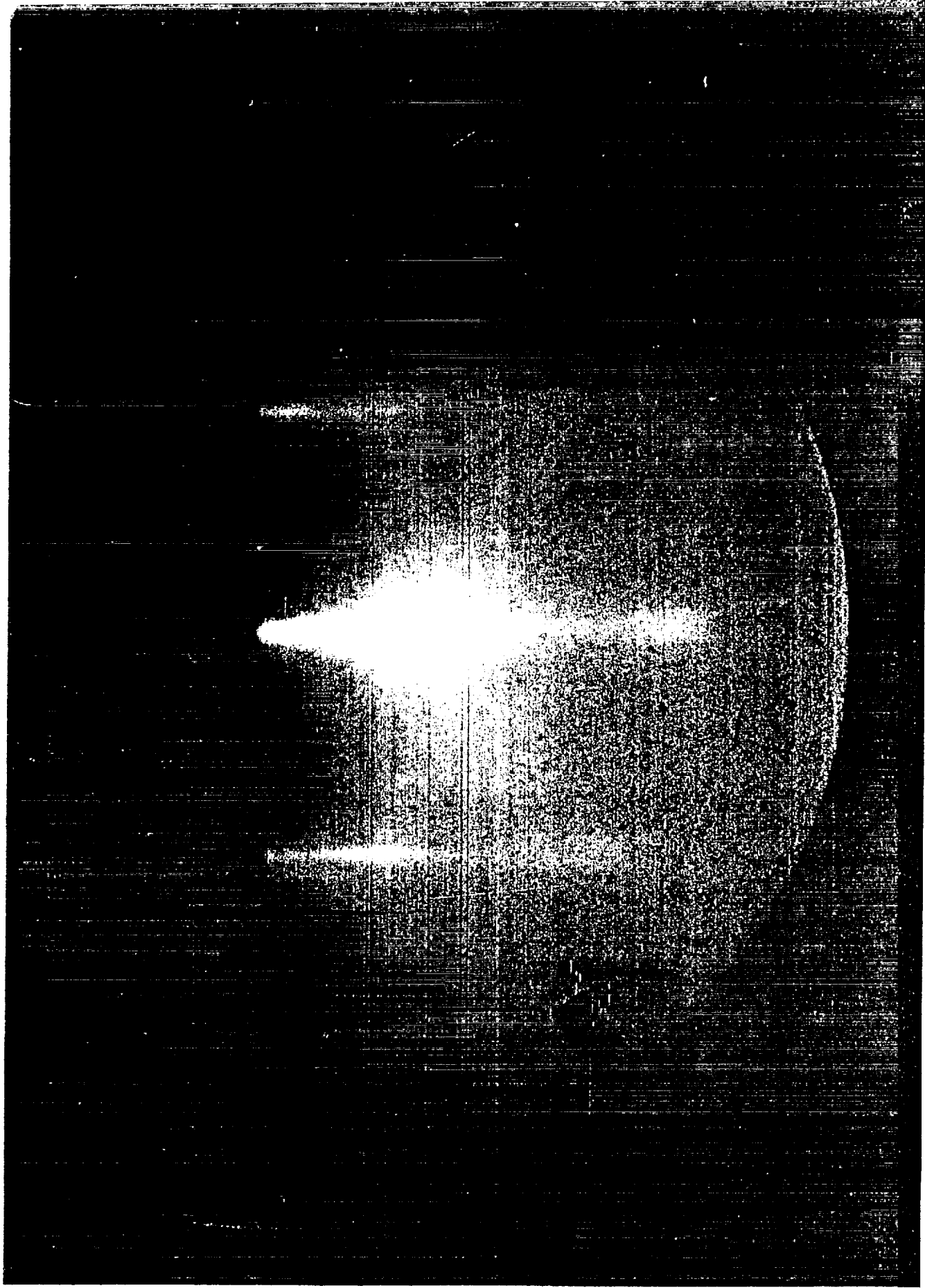


Fig. 9a

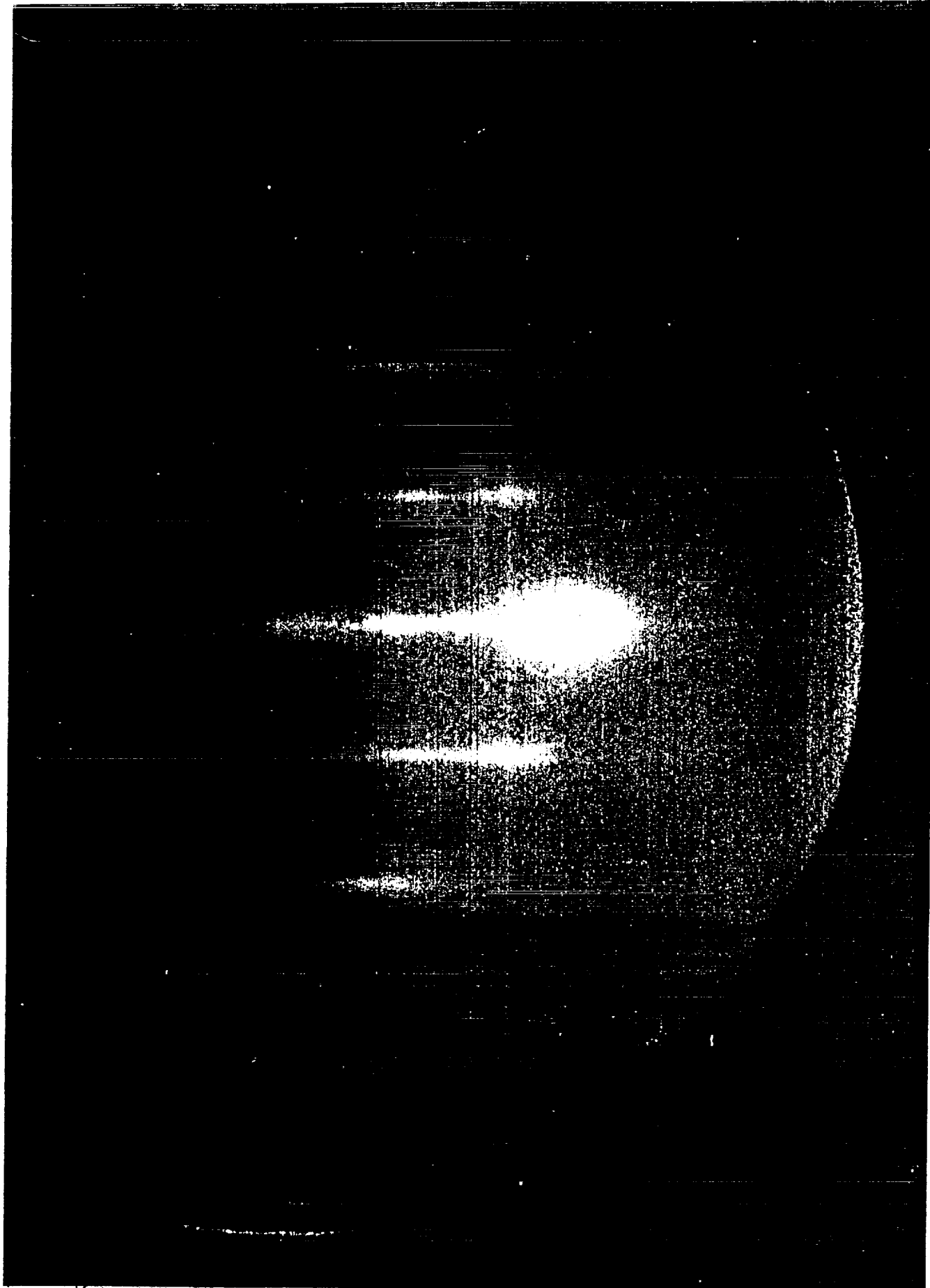
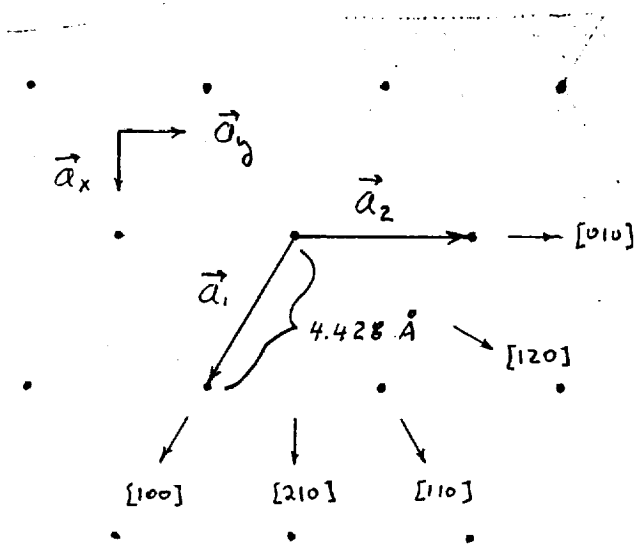


Fig. 96

THE CrSi_2 (001) FACE

CRYSTALLINE
NET



RECIPROCAL
NET

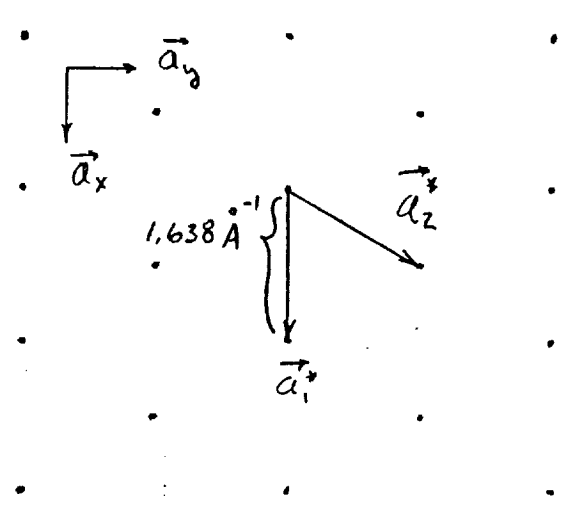


Fig. 10

AN ALTERNATIVE COMMON UNIT MESH
TYPE B

